JOURNAL OF AGRICULTURAL AND FOOD CHEMISTRY
ARTICLE

J. Agric. Food Chem. 2010, 58, 11501–11509 11501
DOI:10.1021/jf101963b

Transepithelial Transport and Metabolism of New Lipophilic Ether Derivatives of Hydroxytyrosol by Enterocyte-like Caco-2/TC7 Cells

Gema Pereira-Caro,[†,‡] Raquel Mateos,*[,†,§] Shikha Saha,[†] Andres Madrona,[#] José Luis Espartero,[#] Laura Bravo,[§] and Paul A. Kroon[†]

[†]Institute of Food Research, Plant Natural Products and Health, Norwich Research Park, Colney Lane, Norwich NR4 7UA, United Kingdom, [‡]IFAPA Centro Venta del Llano, Bailen-Motril, Km 18.5, E-23620 Mengíbar (Jaén), Spain, [§]CSIC, ICTAN-Instituto del Frío, C/José Antonio Novais 10, Ciudad Universitaria, E-28040 Madrid, Spain, and [#]Faculty of Pharmacy, University of Seville, C/Prof. García González 2, 41012 Sevilla, Spain

Intestinal transport and metabolism of a series of ether derivatives of the natural antioxidant hydroxytyrosol with differing alkyl chain lengths (methyl, ethyl, propyl, and butyl) were evaluated at 1, 2, and 4 h using a two-compartment transwell system containing human enterocyte (differentiated Caco-2/TC7) monolayers, which simulates the small intestinal barrier. All four ether derivatives were transferred across the enterocyte monolayers with $P_{app(apical\text{-}basolateral)}$ values between 32.6 and 43.5 cm/s $\times$ 10^{-6}. One hour after apical loading, the predominant forms of the compounds on the basolateral side were unmodified molecules. Glucuronides and methylated metabolites were also present in both the apical and basolateral compartments, with conjugated metabolites preferentially transported to the basolateral side. The rate of metabolism increased according to the lipohilicity of the ether derivative (butyl > propyl > ethyl > methyl). In conclusion, hydroxytyrosyl ethers are rapidly absorbed across, and partially metabolized by, Caco-2/TC7 cell monolayers, in keeping with their lipophilic nature.

KEYWORDS: Phenols; hydroxytyrosol; transephitelial transport; metabolism; Caco-2/TC7 cell monolayer; LC-MS analysis

INTRODUCTION

Hydroxytyrosol (**1**, **Figure 1**), the major phenolic compound present in virgin olive oil, is a bioactive compound that possesses numerous beneficial properties for human health. In this respect, several studies have demonstrated its activity in the prevention of cardiovascular diseases, showing protective effects against oxidation of low-density lipoprotein (*1*), prevention of endothelial dysfunction (*2*), inhibition of platelet aggregation (*3*), and anti-inflammatory activities (*4*). Furthermore, hydroxytyrosol (**1**) has been shown to induce a wide range of antitumor effects, including suppression of proliferation and induction of apoptosis in human colon carcinoma cells (*5*,*6*). In addition, further studies have shown the ability of hydroxytyrosol (**1**) to protect against oxidative stress through its ability to scavenge several radical species (*7*,*8*) and to induce antioxidant enzymes (*9*).

To understand the physiological effects of bioactive compounds such as hydroxytyrosol (**1**), it is necessary to understand how effectively it is absorbed from the intestine and what metabolism it undergoes during this process. Previous studies have shown that hydroxytyrosol (**1**), a rather polar compound, is absorbed in a dose-dependent manner in the small intestine, metabolized in the body, and recovered in both plasma and urine. The majority of the compound is recovered as *O*-glucuronidated conjugates, together with *O*-methyl and monosulfated forms (*10*−*13*) after virgin olive oil administration. These observations indicate that hydroxytyrosol (**1**) is highly bioavailable and undergoes extensive modification during first-pass metabolism, that is, classic phase II biotransformation by the small intestine and liver (*14*).

Tighter regulation of the use of additives in foods, particularly within the European Union, is leading toward significant reductions in the number of antioxidants available for use as food preservatives. In particular, there are likely to be very few lipophilic antioxidants that can be used in foods because concerns that current synthetic compounds such as butylated hydroxyanisole (BHA), butylated hydroxytoluene (BHT), tertiary butylhydroquinone (TBHQ), and propyl gallate (PG) are not safe may lead to their being banned. Currently available natural lipophilic antioxidants are tocopherols (e.g., vitamin E) and β-carotene. There is significant interest in the food industry in the development of new lipophilic antioxidants for use as functional ingredients for incorporation into lipidic food matrices. This is a challenge for food scientists because most phytochemicals with antioxidant activity are hydrophilic. To find useful alternatives to synthetic additives, a series of hydrophobic derivatives (hydroxytyrosyl ethers, **2**−**5**, **Figure 1**) of a natural hydrophilic antioxidant, hydroxytyrosol, were synthesized (*15*). These derivatives

*Corresponding author (phone +0034 915492300; fax +0034 915493627; e-mail raquel.mateos@if.csic.es).

Published on Web 10/07/2010

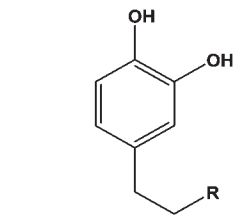

R	Name	Symbol
OH	Hydroxytyrosol	1
OCH_3	Hydroxytyrosyl methylether	2
OC_2H_5	Hydroxytyrosyl ethylether	3
OC_3H_7	Hydroxytyrosyl propylether	4
OC_4H_9	Hydroxytyrosyl butylether	5

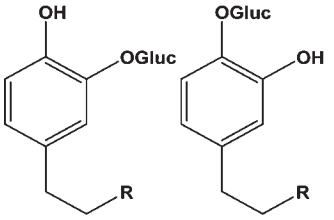

R	Name	Symbol
OCH_3	Monoglucuronide conjugate of **2**	M1
OC_2H_5	Monoglucuronide conjugate of **3**	M3
OC_3H_7	Monoglucuronide conjugate of **4**	M5/M6
OC_4H_9	Monoglucuronide conjugate of **5**	M9/M10

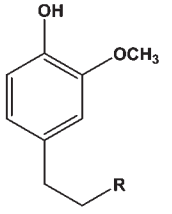

R	Name	Symbol
OCH_3	Monomethyl conjugate of **2**	M2
OC_2H_5	Monomethyl conjugate of **3**	M4
OC_3H_7	Monomethyl conjugate of **4**	M8
OC_4H_9	Monomethyl conjugate of **5**	M11

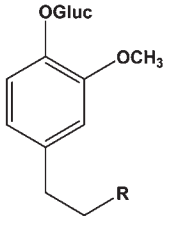

R	Name	Symbol
OCH_3	Methylglucuronide conjugate of **2**	--
OC_2H_5	Methylglucuronide conjugate of **3**	--
OC_3H_7	Methylglucuronide conjugate of **4**	M7
OC_4H_9	Methylglucuronide conjugate of **5**	--

Figure 1. Chemical structures of hydroxytyrosol (**1**), hydroxytyrosyl ethers (**2**−**5**), and their phase 2 metabolites formed after incubation with Caco-2 cells.

were shown to possess higher antioxidant capacity than their precursor, hydroxytyrosol (*16*), and have potential to be developed as bioactive ingredients for the formulation of functional foods or the development of new products with health benefits for consumers.

Because the in vivo biological activity of bioactive dietary components is determined by the extent to which they are absorbed from the gut and metabolized, the intestinal transport and metabolism of hydroxytyrosyl methyl (**2**), ethyl (**3**), propyl (**4**), and butyl (**5**) ethers were investigated. Human intestinal Caco-2/TC7 cell monolayers were used as a useful and predictive model system for intestinal epithelial absorption and metabolism. The intestinal absorption characteristics of the series of ether derivatives (**2**−**5**) are described and related to the hydrophobicity of the derivatives. In addition, the extent of phase 2 metabolism and the nature of the metabolites are described.

MATERIALS AND METHODS

Materials. All cell culture media and reagents were from Invitrogen (Paisley, U.K.) unless otherwise stated. Enzymes (catechol-*O*-methyltransferase, β-glucuronidase from *Helix pomatia*, and sulfatase type V from limpets), *S*-adenosyl-L-methionine chloride, UDP-glucuronic acid, and adenosine-3′-phospho-5′-phosphosulfate were purchased from Sigma Chemical Co. (Poole, Dorset, U.K.). Methanol and formic acid were acquired from Fisher Scientific (Loughborough, U.K.) and Sigma-Aldrich, respectively. Hydroxytyrosyl ethers (**2**−**5**) were prepared by chemical synthesis from hydroxytyrosol (**1**) (*15*) and further purified by column chromatography to yield practically pure compounds (> 98% purity). Standards of methyl derivatives were obtained by chemical synthesis from homovanillyl alcohol (*17*). All reagents were of analytical or chromatographic grade.

Human Colon Adenocarcinoma Cells Culture. The human Caucasian colon adenocarcinoma cell line Caco-2 (TC7 clonal cells) was a kind gift from Dr. Monique Rousset (INSERM, Paris, France). Caco-2/TC7 cells were grown in 75 cm^2 flasks and maintained in Dulbecco modified Eagle's medium (DMEM) (without phenol red) supplement with 20% fetal calf serum, 1% (v/v) nonessential amino acids, 2 mmol/L glutamine, 100 IU/mL penicillin, and 100 μg/L streptomycin in a humidified atmosphere of 5% CO_2 and 95% air at 37 °C. All cells used were between passages 50 and 60.

Preparation of Test Solutions. Standard stock solutions (50, 20, and 10 mM) of each compound were prepared in 10% DMSO in deionized water. Then, 10 and 100 times diluted solutions were prepared from stock solutions by adding distilled water providing the following range of concentrations (5000, 2000, 1000, 500, 200, 100, 50, 20, and 10 μM, 1% DMSO) to ultimately dilute them with serum-free DMEM supplemented with 200 μM ascorbic acid to prepare test solutions (500, 200, 100, 50, 20, 10, 5, 2, and 1 μM, 0.1% of DMSO). Concentrations were checked by HPLC to confirm their complete dissolution in aqueous DMEM media.

Evaluation of Cytotoxicity. The effect of hydroxytyrosyl ether (**2**−**5**) on Caco-2/TC7 cell proliferation was evaluated using a WST-1 cell proliferation kit (catalog no. 11 644 807 001, Roche Applied Science,

Germany). The WST-1 (4-[3-(4-iodophenyl)-2-(4-nitrophenyl)-2*H*-5-tetrazolio]-1,3-benzene disulfonate) reagent was used according to the kit specifications. Briefly, Caco-2/TC7 cells were plated in 96-well culture plates in a final volume of 100 μL/well culture medium (7.2×10^4 cells/well) in a humidified atmosphere (37 °C, 5% CO_2). Cells were allowed to adhere to the plate surface for 36 h before being exposed to various concentrations of hydroxytyrosyl ethers (**2**−**5**) (1, 2, 5, 10, 20, 50, 100, 200, and 500 μM; 0.1% DMSO final concentration) for 24 h. Each dose of polyphenols was tested six times. Then, 10 μL of cell proliferation reagent, WST-1, dissolved in serum-free DMEM, was added to each well after removal of phenolics solutions and washing cells with PBS, and was incubated for 90 min in a humidified atmosphere (37 °C, 5% CO_2). Quantification of the formazan dye produced by metabolically active cells was performed by a scanning multiwell spectrophotometer, measuring absorbance at 450 nm by microplate ELISA reader (ELx808, Ultra Microplate Reader; Bio-Tek Instruments, Inc., Winooski, VT) after the plate had been shaken thoroughly for 1 min. Results are expressed as percentages of cell viability, which was calculated on the basis of the absorbance measurement obtained for cells exposed to the culture medium as a control.

Transport and Metabolism Experiments. Caco-2/TC7 cells were grown in Transwell inserts with the semipermeable membrane first coated with type I collagen (12 mm diameter and 0.4 μm pore size, Corning Costar, Corning, NY). The cells were seeded at a density of $(2-4) \times 10^4$ cells/cm^2, and the monolayers were formed after culturing for 21 days postconfluence. The integrity of the cell monolayers was evaluated by measurement of transepithelial electrical resistance (TEER) with Millicel-ERS volt ohmmeter equipment (Millipore Corp., Billerica, MA). Monolayers with a TEER ≥ 200 Ω cm^2 were used for the transepithelial transport experiments. Additionally, TEER measurements were taken before and after experiments to ensure adequate monolayer integrity. Moreover, the barrier integrity of Caco-2/TC7 monolayers was determined by quantifying the transfer of a 100 μM solution of phenolsulfonaphthalein (phenol red), a marker of paracellular flux, from the apical compartment to the basolateral compartment and vice versa, after incubation for 60 min at 37 °C. Wells that supported < 0.1% of phenol red transport under these conditions were considered to be suitable for use. Stock solutions of hydroxytyrosyl ethers (**2**−**5**) were dissolved in 10% of DMSO in deionized water and diluted with serum-free DMEM supplemented with 200 μM ascorbic acid to prepare test solutions (50 μM; 0.1% DMSO) to prevent potential oxidation of the antioxidant compounds. The resulting 0.1% final concentration of DMSO and 200 μM ascorbic acid present in the test solutions were equivalent to those used in control and did not affect the transport and metabolism experiments.

Hydroxytyrosyl Ether (**2**−**5**) *Metabolism Experiments.* Hydroxytyrosyl ethers (**2**−**5**) test solutions (50 μM; 0.1% DMSO) were apically added to each well, with the equivalent volume of DMSO as control. All solutions contained 200 μM ascorbic acid as a protective antioxidant. Control and treated cells were incubated at 37 °C for 1, 2, and 4 h. Media from apical and basolateral sides were taken and kept at −20 °C until their analysis. Cells were washed twice with PBS (0.01 M phosphate buffered saline solution, pH 7.4) and harvested by scraping. After centrifugation at 1500 rpm for 5 min at 4 °C, the supernatant was removed and the cell pellet resuspended in 200 μL of PBS. Cells were sonicated for 10 min at room temperature to break down the cell membrane and to release the total amount of metabolites. After centrifugation at 5000 rpm for 10 min at 4 °C, the supernatant was transferred into an Eppendorf vial and kept frozen at −20 °C. Pellets obtained were redissolved in methanol and centrifuged at 5000 rpm for 10 min at 4 °C to check for the presence of these compounds and/or their metabolites in the cellular membranes. Media, cytoplasmatic content, and methanolic extracts were subjected to HPLC and LC-MS analyses. All metabolic experiments were run in triplicate.

Identification of Hydroxytyrosyl Ether (**2**−**5**) *Conjugates.* In vitro glucuronidation and sulfatation of hydroxytyrosyl derivatives (**2**−**5**) were carried out. Standard solutions of hydroxytyrosyl ethers (**2**−**5**) were enzymatically conjugated in vitro using a rat liver microsomal fraction that contained both UDP-glucuronosyltransferase (UGT) and sulfotransferase (*18*). The preparation of microsomal fractions from liver was done according to the procedure described by Graham et al. (*19*) and previously used by our group with some modifications (*20*). Standards of methyl derivatives were obtained by chemical synthesis from homovanillyl alcohol (*17*).

Media and cell fractions were subjected to HPLC analysis following incubation with sulfatase and β-glucuronidase enzymes. Enzymatic hydrolysis of conjugates detected in media samples was carried out by the addition of 0.23 mg (150 units) β-glucuronidase (645,200 units/g) or 10 mg (150 units) of sulfatase type V from limpets (15,000 units/g). Subsequently, a 1 mL portion of enzyme-treated sample was mixed with 50 μL of trifluoracetic acid and 50 μL of methanol. Samples were centrifuged at 13.000*g* for 10 min before the supernatants were injected onto the HPLC.

Hydroxytyrosyl Ether (**2**−**5**) *Transport Experiments.* To measure the apical-to-basolateral permeability, 0.6 mL of the test solution containing hydroxytyrosyl ethers (**2**−**5**) (50 μM; 0.1% DMSO, 200 μM ascorbic acid) was added to the apical side while the basolateral chamber of the Transwell insert was filled with 1.5 mL of serum-free DMEM with ascorbic acid (200 μM). However, to measure the basolateral-to-apical transport, 1.5 mL of the test solution containing the polyphenols (hydroxytyrosyl ethers (**2**−**5**)) and 200 μM ascorbic acid was added to the basolateral side while the apical side was filled with 0.6 mL of serum-free DMEM with ascorbic acid (200 μM). Plates were incubated in a humidified atmosphere of 5% CO_2 at 37 °C during 1, 2, and 4 h. Two controls without DMSO and with the equivalent volume of DMSO (0.1%) were monitored. Media from the apical and basolateral sides and harvested cells were kept at −20 °C until their later analysis by HPLC. The apparent permeability coefficient (P_{app}, cm/s) for parent compounds after 1 h of incubation with cells in both directions as well as the efflux ratio was determined. Besides, the rate of individual conjugate efflux for both the apical and basolateral compartments was calculated, and these rates were used to determine an apical to basolateral ratio. This ratio is a measure of the favored direction of efflux, with values > 1.0 indicating an apically favored efflux, values < 1.0 symbolizing basolaterally favored efflux, and values of 1.0 representing an equal distribution of conjugate efflux. Percentages of parent compounds or metabolites of hydroxytyrosyl ethers (**2**−**5**) found in apical and basolateral sides after 1, 2, and 4 h of incubation with Caco-2/TC7 cells were also offered to know their behavior over time. All assays were run in triplicate.

HPLC Analysis. All extracellular culture samples and cell lysates from metabolism and transport experiments of hydroxytyrosyl ethers (**2**−**5**) by Caco-2/TC7 cell monolayers were analyzed on an Agilent 1100 liquid chromatographic system equipped with a diode array UV−vis detector and a thermostat autosampler (4 °C, 50 μL injection volume). A 250 mm × 4.6 mm i.d., 5 μm particle size Phenomonex Luna C18 column was used. An Agilent ChemStation software system controlled the equipment and carried out data processing. Elution of samples was performed at a flow rate of 1.0 mL/min at 37 °C, using as mobile phase of water (solvent A) and methanol (solvent B), both with 0.1% formic acid. The solvent gradient for hydroxytyrosyl ethyl (**3**), propyl (**4**), and butyl (**5**) ethers changed according to the following conditions: from 100 to 90% A in 5 min; 85% A in 5 min; 65% A in 10 min; 60% A in 10 min; 55% A in 5 min; 50% A in 5 min; 30% A in 5 min; 0% A in 5 min, followed by 5 min of maintenance and 100% A in 5 min. For hydroxytyrosyl methyl ether (**2**) the gradient program was as follows: from 100 to 90% A in 5 min; 85% A in 5 min; 65% A in 10 min; 60% A in 15 min; 55% A in 5 min; 50% A in 5 min; 0% A in 5 min; followed by 5 min of maintenance and 100% A in 5 min. Chromatograms were acquired at 280 nm. Synthetic hydroxytyrosyl ethers (**2**−**5**) and monomethyl hydroxytyrosyl ethers (*17*) were used for quantification purposes. Standards of the parent compounds were prepared in serum-free DMEM culture media in a range of concentrations from 1 to 50 μM, obtaining a linear response for all standard curves, as checked by linear regression analysis with R^2 values of > 0.99 ($n = 6$). The recoveries from standards added to the culture medium ranged from 90.3 to 100%, and detection and quantification limits varied from 0.2 to 0.6 μM and from 0.8 to 1.9 μM, respectively. The precision of the assay was between 99.2 and 99.6% (as the coefficient of intra-assay variation), allowing the quantification of hydroxytyrosyl ethers (**2**−**5**) and their metabolites, quantified as equivalents of the respective parent molecule except methyl derivatives, which had their own reference.

Liquid Chromatography−Mass Spectrometry. Following HPLC-DAD analysis, a subset of samples was then injected onto an HPLC-electrospray ionization (ESI)-MS system for structural elucidation using

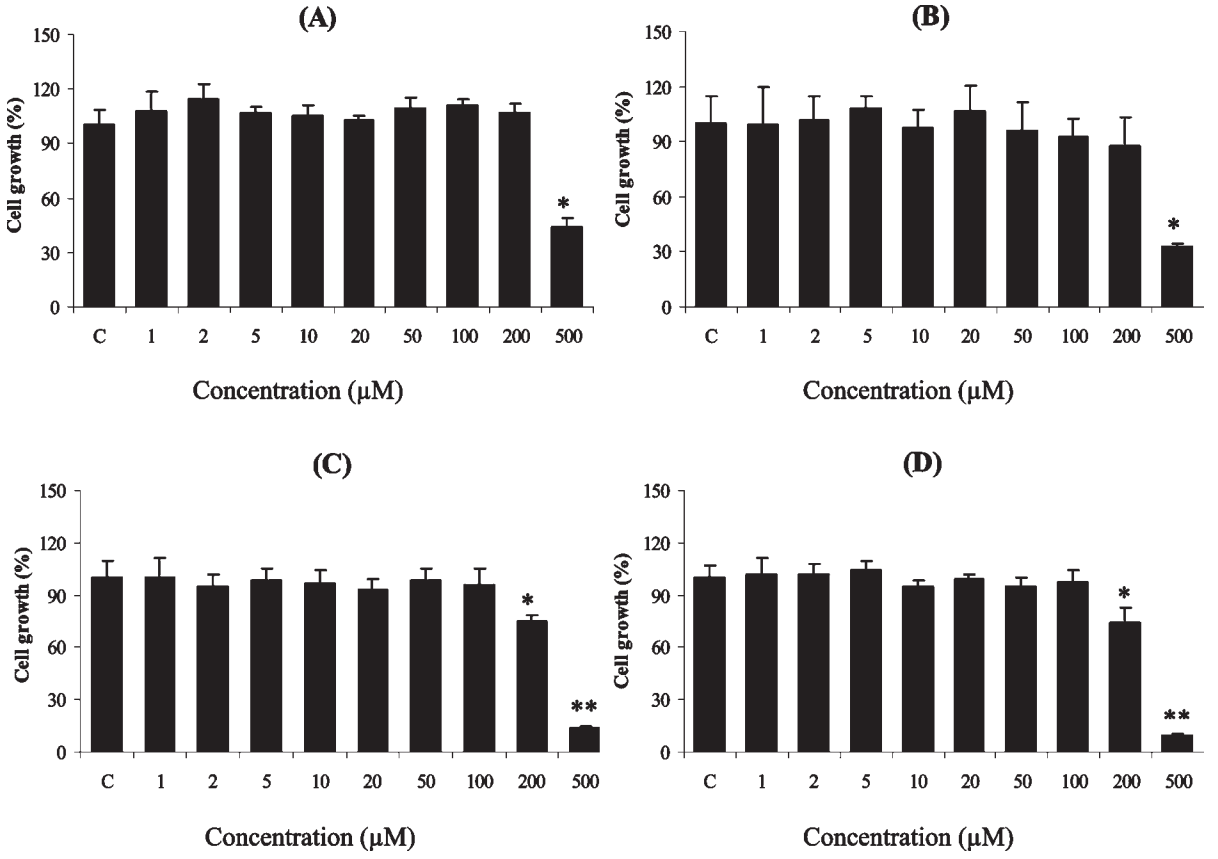

Figure 2. Effects of hydroxytyrosyl ether (**2**−**5**) treatment for 24 h on Caco-2/TC7 cytotoxicity measured using the WST-1 assay: (**A**) hydroxytyrosyl methyl ether (**2**); (**B**) hydroxytyrosyl ethyl ether (**3**); (**C**) hydroxytyrosyl propyl ether (**4**); (**D**) hydroxytyrosyl butyl ether (**5**), in a range of concentrations between 1 and 500 μM. Values presented are means ± SD of six determinations. *, $p < 0.05$ compared with untreated cells (control cells); **, $p < 0.05$ compared with treated cells.

an Agilent 1100 series HPLC-DAD coupled to an Agilent 1100 series Agilent LC/MSD SL single-quadrupole mass spectrometer (Micromass, Manchester, U.K.). MS detection was performed in full scan mode (mass range, 100−1000 Da) with the following spray chamber conditions: drying gas (N_2) flow of 13 L/min; nebulizer pressure of 50 Psi; and drying gas temperature of 350 °C. A positive ionization mode was used to analyze all polyphenols and conjugates at a capillary voltage of 4000 V and a fragmentor setting of 100. HPLC conditions (eluents, column, flow rate, gradient, etc.) were as stated above.

Statistical Analysis. Results are expressed as mean ± standard deviation (SD) of three measurements obtained from three independent experiments. Data were subjected to a nonparametric one-way analysis of variance (Kruskal−Wallis test) using the SPSS 17.0 program. Differences were considered to be significant when $p < 0.05$.

RESULTS

Cytotoxic Evaluation of Hydroxytyrosyl Ethers (2−5) after Exposure to Caco-2/TC7 Cells. The effect of the hydroxytyrosyl ethers (**2**−**5**) on the Caco-2 cells was assessed after the cells had been treated with various concentrations (1, 2, 5, 10, 20, 50, 100, 200, and 500 μM) of hydroxytyrosyl ethers for 24 h. Subsequently, the number of viable cells was measured using the WST-1 assay; data are depicted in **Figure 2**. In general, there were no differences in cell viability after 24 h between treated and control cells at concentrations up to 200 μM for hydroxytyrosyl methyl (**2**) and ethyl (**3**) ethers or at 100 μM for hydroxytyrosyl propyl (**4**) and butyl (**5**) ethers. However, these compounds showed 43.7, 32.6, 13.9, and 9.50% Caco-2/TC7 viabilities at 500 μM concentration after 24 h of treatment for hydroxytyrosyl methyl (**2**), ethyl (**3**), propyl (**4**), and butyl (**5**), respectively. This shows a direct relationship between the lipophilic nature of the tested compounds and a decreased cell viability, although this cytotoxic effect is only apparent at high concentrations. Because there was no cytotoxic effect observed at 50 μM for any of the compounds, this concentration was selected for use in the transport and metabolism experiments.

Identification of Hydroxytyrosyl Ether (2−5) Conjugates. When hydroxytyrosyl ethers (**2**−**5**) were added apically to a final concentration of 50 μM (0.1% DMSO; 200 μM ascorbic acid), HPLC analysis of cell culture media from Caco-2/TC7 cells incubated with these polyphenols resulted in the appearance of a number of peaks with absorbance at 280 nm that were not present in the untreated control media. In addition, the concentration of the hydroxytyrosyl ethers (**2**−**5**) themselves decreased; taken together, these observations suggest that the additional peaks were metabolites of the original polyphenols (**Figure 3**). All of the new peaks were sufficiently separated from peaks that were present in the culture media of control cells, which facilitated the identification of individual metabolites of the hydroxytyrosyl alkyl ethers that appeared after incubation in the presence of cells.

The following approaches were used to gain information about metabolite structure: comparison of retention times and spectral characteristics with authentic hydroxytyrosyl alkyl ether standards; analysis by electrospray ionization mass spectrometry in positive mode with selected ion monitoring (SIM); hydrolysis with β-glucuronidase or aryl sulfatase or a mixture of both; and in vitro conjugation (rat liver microsomes) of hydroxytyrosyl alkyl ether standards and comparison with test samples.

Identification of Hydroxytyrosyl Methyl Ether (*2*) *Conjugates*. Media from hydroxytyrosyl methyl ether (**2**) treated cells yielded two new peaks at 20.6 and 31.2 min labeled M1 and M2, respectively, together with the original compound **2** at 21.6 min (**Figure 3A**). Their UV spectra showed a peak around 270−280 nm,

characteristic of *o*-diphenolic compounds. Enzymatic hydrolysis using β-glucuronidase of media from hydroxytyrosyl methyl ether (**2**) treated cells resulted in a significant reduction of peak M1 with an increase in peak size for the parent compound (**2**). LC-MS analysis indicated the presence of the molecular ion at *m*/*z* 345.1 and fragment ion at *m*/*z* 137.1 corresponding to the dehydrated hydroxytyrosol (**Table 1**). All results together with the in vitro glucuronidation of parent compound **2** confirmed the identity of M1 as a monoglucuronide conjugate of hydroxytyrosyl methyl ether (**2**). Identification of M2 at 31.2 min (**Figure 3A**) was carried out by comparing the spectral characteristics and retention time with those of an authentic standard and indicated it was a monomethyl conjugate of **2**. Furthermore, the methyl conjugate of hydroxytyrosyl methyl ether (**2**) was confirmed by LC-MS, showing a molecular ion $[M + H]^+$ at *m*/*z* 183.1, plus a fragment ion at *m*/*z* 151.1 corresponding to the protonated molecular ion and dehydrated monomethyl conjugate, respectively (**Table 1**).

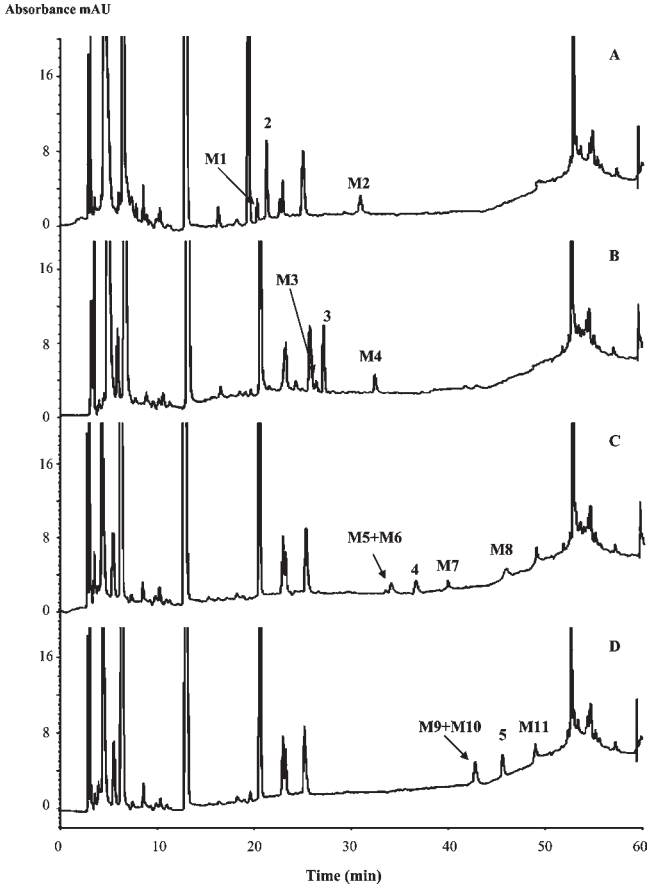

Figure 3. Typical profile of the chromatographic separation of different molecular species detectable in medium from Caco-2/TC7 cells in culture after 2 h of incubation with 50 μM concentration of the following compounds: (**A**) hydroxytyrosyl methyl ether (**2**); (**B**) hydroxytyrosyl ethyl ether (**3**); (**C**) hydroxytyrosyl propyl ether (**4**); (**D**) hydroxytyrosyl butyl ether (**5**). For peak identification, see **Table 1**.

Identification of Hydroxytyrosyl Ethyl Ether (***3***) *Conjugates*. Two new peaks at 26.4 and 32.4 min, labeled M3 and M4, respectively, were identified as potential metabolites after incubation of hydroxytyrosyl ethyl ether (**3**) with Caco-2/TC7 (**Figure 3B**). M3 was identified as a monoglucuronide of **3** on the basis of its being hydrolyzed when treated with β-glucuronidase and its coeluting and having the same MS fragmentation as a monoglucuronide metabolite obtained biosynthetically (molecular ion $[M + H]^+$ at *m*/*z* 359.1 and a fragment ion at *m*/*z* 137.1 corresponding to the protonated molecular ion and dehydrated hydroxytyrosol, respectively). Analysis of peak M4 based on its comparison with a synthetic standard, a monomethyl conjugate of **3**, together with data from the LC-MS analysis of samples obtained after hydroxytyrosyl ethyl ether (**3**) incubation (**Table 1**), permitted its identification as a monomethyl conjugate of **3**.

Identification of Hydroxytyrosyl Propyl Ether (***4***) *Conjugates*. Samples from the incubation of this compound with Caco-2/TC7 cells generated four new peaks at retention times of 33.8, 34.3, 40.2, and 46.0 min (labeled M5, M6, M7, and M8, respectively) (**Figure 3C**). Peaks M5, M6, and M7 disappeared after β-glucuronidase treatment with the subsequent increase of compound **4** and peak M8. In vitro synthesis of glucuronides of **4** provided two chromatographic peaks, M5 and M6, for which LC-MS analysis showed a molecular ion $[M + H]^+$ at *m*/*z* 373.2 and a fragment ion at *m*/*z* 137.1. All of this information allowed the identification of M5 and M6 as monoglucuronides of hydroxytyrosyl propyl ether (**4**); these are almost certainly the 3- and 4-monoglucuronides of hydroxytyrosyl propyl ether. M8 was coincident in retention time with the synthetic monomethyl derivative of **4**, the spectroscopic characteristics and LC-MS analysis of which, detailed in **Table 1**, confirmed its identity as a monomethyl conjugate of hydroxytyrosyl propyl ether (**4**). Finally, M7 was hydrolyzed upon treatment with β-glucuronidase with a concomitant increase in M8; taken together with data from the analysis by LC-MS, M7 was identified as a methylglucuronide of **4**.

Identification of Hydroxytyrosyl Butyl Ether (***5***) *Conjugates*. Three distinct peaks at 42.4, 42.6, and 48.9 min (labeled M9, M10, and M11, respectively) were detected as potential metabolites (**Figure 3D**). Following the same approach as

Table 1. Chromatographic and Spectroscopic Characteristics of Hydroxytyrosyl Methyl (**2**), Ethyl (**3**), Propyl (**4**), and Butyl (**5**) Ethers and the Formed Metabolites after Their Incubation with Caco-2/TC7 Cell Monolayers

compd	MW	RT (min)	λ_{max}	$[M + H]^+$ (*m*/*z*)	fragment ion (*m*/*z*)	proposed structure
2	168.2	21.6	280	169.1	137.1	hydroxytyrosyl methyl ether
M 1	344.2	20.6	278	345.1	137.1	monoglucuronide of **2**
M2	182.2	31.2	280	183.1	151.1	monomethyl conjugate of **2**
3	182.2	27.8	280	183.0	137.1	hydroxytyrosyl ethyl ether
M3	358.2	26.4	278	359.2	137.1	monoglucuronide of **3**
M4	196.2	32.4	280	197.2	151.2	monomethyl conjugate of **3**
4	196.2	36.8	282	197.2	137.1	hydroxytyrosyl propyl ether
M5/M6	372.2	33.8/34.3	280	373.2	137.1	monoglucuronide of **4**
M7	386.2	40.2	278	387.2	151.1	methylglucuronide of **4**
M8	210.2	46.0	282	211.2	151.1	monomethyl conjugate of **4**
5	210.1	45.6	280	211.0	137.1	hydroxytyrosyl butyl ether
M9/M10	386.1	42.4/42.6	278	387.0	137.1	monoglucuronide of **5**
M11	224.1	48.9	280	225.2	151.1	monomethyl conjugate of **5**

Table 2. P_{app} and Efflux Ratio (ER, AP/BL) Values for Hydroxytyrosyl Ethers (**2**−**5**)[a]

compd	$P_{app\ AP\rightarrow BL}$ (cm/s × 10^{-6})	$P_{app\ BL\rightarrow AP}$ (cm/s × 10^{-6})	ER
2	32.6 ± 2.2 a	27.1 ± 1.8 b	1.2 ± 0.1 a
3	33.4 ± 0.4 a	22.3 ± 2.3 a	1.5 ± 0.1 b
4	32.6 ± 1.1 a	24.0 ± 0.5 a	1.4 ± 0.1 b
5	43.5 ± 1.1 b	22.5 ± 0.5 a	1.9 ± 0.1 c

[a] AP→BL indicates apical to basolateral transport. BL→AP indicates basolateral to apical transport. ER values are from (P_{app} AP→BL/P_{app} BL→AP). Values are expressed as mean ± SD of three determinations, where all values within a column with different letters are significantly different ($p < 0.05$).

described above, M9 and M10 were shown to correspond to monoglucuronide derivatives, whereas M11 was shown to be the monomethyl derivative of hydroxytyrosyl butyl ether (**5**), in agreement with synthetic standard spectral characteristics summarized in **Table 1**.

In general, for the monoglucuronide conjugates, we could not distinguish between structural isomers (e.g., 3-hydroxy-4-glucuronide-phenylethanol or 3-glucuronide-4-hydroxyphenylethanol). However, the methyl derivatives that were identified corresponded to a series of homovanillyl ethers.

Transepithelial Hydroxytyrosyl Ethers (2−5) Transport through Differentiated Caco-2/TC7 Cell Monolayers. A preliminary study showed that hydroxytyrosyl ethers (**2**−**5**) were stable (> 98% recovery) in serum-free DMEM medium containing 200 μM ascorbic acid in the absence of cells for up to 24 h at 37 °C. In addition, preliminary experiments in our laboratory proved that concentrations of ascorbic acid up to 1000 μM can be safely used because no cytotoxic effect was observed after incubation with Caco-2 cells (data not shown). To evaluate the transport of hydroxytyrosyl ethers (**2**−**5**) and their metabolites through the Caco-2 monolayers, 50 μM concentrations of parent compounds were loaded both apically and basolaterally in independent experiments, to determine the apical (AP) to basolateral (BL) and the BL to AP transport. The apparent permeability coefficient (P_{app}, cm/s) both from AP to BL and from BL to AP directions was calculated using data from 1 h incubations with Caco-2/TC7 cells because linearity of bidirectional transport across Caco-2 monolayers is observed with shorter incubation periods during which metabolized and transported compounds account for only a fraction of the total applied (*21*). P_{app} values for both directions and efflux ratios (ER) ($P_{app\ AP\rightarrow BL}$/$P_{app\ BL\rightarrow AP}$) corresponding to the hydroxytyrosyl ethers (**2**−**5**) are displayed in **Table 2**. The results indicated that all four compounds were transported in both directions and that AP to BL transport was more rapid than BL to AP transport. Hence, the ER values are >1.0, indicating a good permeability of hydroxytyrosyl ethers (**2**−**5**) across the Caco-2 cell monolayers. In addition, a direct relationship was observed between the lipophilicity of the hydroxytyrosyl ethers (**2**−**5**) and their ER values.

The transport characteristics of individual hydroxytyrosyl ether (**2**−**5**) conjugates were also determined after 60 min of incubation, and values are expressed as the apical to basolateral transport ratio (**Table 3**). In this context, a value of < 1.0 indicates preferential basolateral transport, whereas a value of > 1.0 indicates preferential apical transport. Total conjugate production was 55.1, 92.2, 177.0, and 195.4 pmol/min for hydroxytyrosyl methyl (**2**), ethyl (**3**), propyl (**4**), and butyl (**5**) ethers, respectively. These results indicate that there is a direct relationship between the lipophilicity of the compound and the metabolic yield during transport across Caco-2/TC7 cell monolayers. In addition, it was observed that hydroxytyrosyl methyl (**2**) and ethyl (**3**) ethers were preferentially methylated (22.7 and 25.7% of methyl conjugates versus 15.6 and 7.4% of glucuronide conjugates in the basolateral side after 4 h of incubation, respectively) during transport across Caco-2/TC7 cells, whereas hydroxytyrosyl propyl (**4**) and butyl ethers (**5**) were preferentially metabolized to glucuronide conjugates rather than methylated derivatives (35.8 and 73.8% of glucuronide conjugates versus 31.0 and 6.6% of methyl conjugates in the basolateral side after 4 h of incubation, respectively) at the assayed concentration of 50 μM. Overall, apical efflux accounted for approximately 5.0% of conjugate efflux, and basolateral efflux accounted for about 95% of efflux. Cellular contents accounted for < 0.1% of the total conjugates within the monolayers in any experiment, whereas no detectable compound was found in the cellular membranes after evaluation of methanolic extracts from the cellular debris, probably because the levels of polyphenols potentially present in cellular membranes are below the limit of detection. All of the detected conjugates demonstrated preferential basolateral transport as indicated by the apical to basolateral ratio values being < 0.08 in all cases.

Table 3. Transport of Individual Hydroxytyrosyl Ethers (**2**−**5**) Conjugates in Caco-2/TC7 Cell Monolayers to the Apical and Basolateral Media[a]

compd	apical transport (nmol/min) × 10^{-3}	basolateral transport (nmol/min) × 10^{-3}	AP/BL ratio
Hydroxytyrosyl Methyl Ether (2) Metabolism			
M1	0.3 ± 0.1	18 ± 7	0.0167
M2	1.8 ± 0.4	35 ± 1	0.0514
TCP[b] (nmol/min)	2.1 (3.8%)	53 (96.2%)	
Hydroxytyrosyl Ethyl Ether (3) Metabolism			
M3	0.2 ± 0.1	11 ± 3	0.0181
M4	5 ± 2	76 ± 2	0.0654
TCP (nmol/min)	5.2 (5.6%)	87 (94.4%)	
Hydroxytyrosyl Propyl Ether (4) Metabolism			
M5/M6	0.8 ± 0.1	42 ± 10	0.0190
M7	3.3 ± 0.5	50 ± 2	0.0660
M8	5.5 ± 0.1	75.4 ± 4.0	0.0770
TCP (nmol/min)	9.6 (5.4%)	167.4 (94.6%)	
Hydroxytyrosyl Butyl Ether (5) Metabolism			
M9/M10	2 ± 1	134.7 ± 0.6	0.0148
M11	3.7 ± 0.5	55 ± 1	0.0672
TCP (nmol/min)	5.7 (2.9%)	189.7 (97.1)	

[a] Values are expressed as mean ± SD of three determinations. [b] TCP, total polyphenols conjugation production.

The proportions of parent compounds or their metabolites present in the AP or BL compartments after 1, 2, and 4 h of incubation with Caco-2/TC7 cells with a starting concentration of 50 μM of the compound are shown in **Figure 4**. Time-dependent transport was observed. For AP to BL transport, it is noteworthy that the percentage of transported nonmetabolized compound ranged between 98.5 and 61.7%, between 72.0 and 66.9%, between 53.8 and 33.2%, and between 46.5 and 19.6% for hydroxytyrosyl methyl (**2**), ethyl (**3**), propyl (**4**), and butyl (**5**) ethers, respectively (ranges cover 1−4 h of incubation). This indicates that a substantial portion of the hydroxytyrosyl alkyl ethers escape metabolism during transport to the basolateral compartment.

DISCUSSION

To provide alternative lipophilic antioxidant additives to the food industry for application in functional foods, a series of new compounds, hydroxytyrosyl alkyl ethers (**2**−**5**), were synthesized from a natural precursor, hydroxytyrosol (**1**), which is a

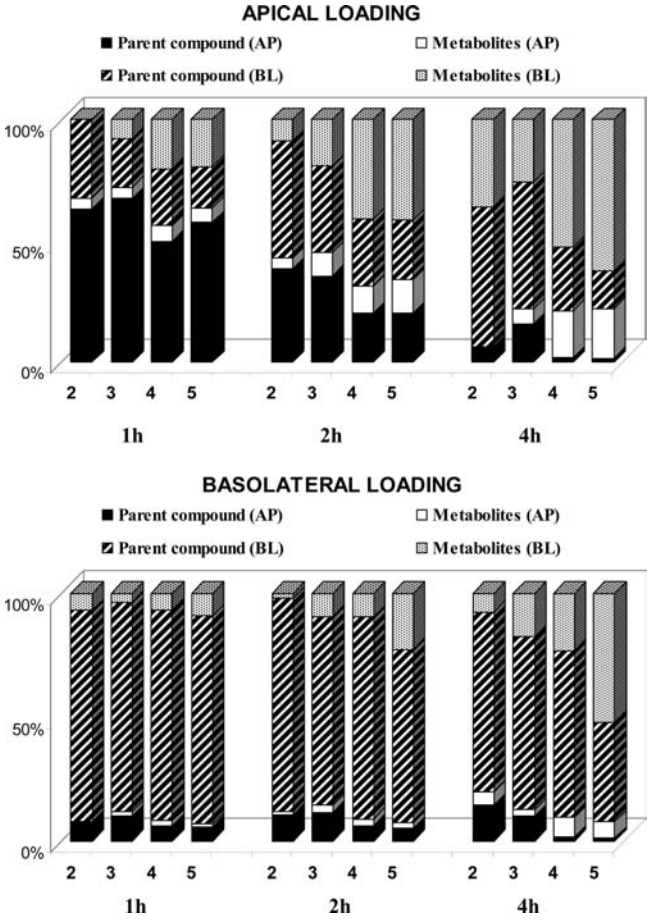

Figure 4. Percentage of hydroxytyrosyl ethers (**2**−**5**) and their metabolites found in apical (AP) and basolateral (BL) sides after 1, 2, and 4 h of incubation with Caco-2/TC7 cells. Results showed a standard deviation of <10%.

characteristic polyphenol of virgin olive oil (*15*). This group of synthetic compounds (**2**−**5**) exhibited similar or even higher antioxidant activities than the parent hydroxytyrosol (*16*). To understand the potential impact of these compounds in vivo, it is important to know the extent to which they are absorbed from the gut and the nature of the compounds after absorption. We used the human intestinal Caco-2 cell transwell model that has been used extensively to characterize the intestinal absorption of a range of drugs, other xenobiotics, and nutrients such as iron. In addition, differentiated Caco-2 cells exhibit phase 2 conjugating enzyme activities and are therefore suitable for assessing the extent of metabolism and for identifying human metabolites. Using the WST-1 assay as a measure of toxicity, it was shown that none of the hydroxytyrosyl alkyl ethers induced significant effects on cell viability at concentrations up to 50 μM. Furthermore, the selection of the most appropriate concentration of hydroxytyrosyl derivatives that has been used to treat the colon cancer cells also considered the concentration of polyphenols achievable for absorption in the intestine from dietary intake. Focusing on olive oil phenols, tyrosol and hydroxytyrosol are absorbed by humans in a dose-dependent manner with the phenolic content of the olive oil administered (*13*). In this context, in the Mediterranean areas a daily consumption of 25−50 mL of virgin olive oil with a concentration range between 180 and 300 mg/kg of olive oil phenols would result in an estimated intake of about 9 mg of olive oil phenols per day. A recent study has shown that a single ingestion of 40 mL of olive oil with high (366 mg/kg) and medium (164 mg/kg) contents of polyphenolic compounds leads to a plasma hydroxytyrosol concentration of around 15−30 μM (*22*). In addition, in a human ileostomy study it was shown that up to 66% of the ingested olive oil phenols were absorbed from the small intestine (*23*). Taking into account these results, 25−45 μM concentrations of phenolic compounds should reach the gut in order to detect 15−30 μM concentrations of these polyphenols in the plasma. On the basis of these results, we selected a 50 μM concentration of each evaluated compound for this study.

The data presented in this paper show that all four hydroxytyrosyl alkyl ethers (**2**−**5**) were efficiently absorbed across the intestinal epithelial monolayers. There was a direct relationship between their lipophilicity and absorption rate, indicated by their efflux ratios ($P_{app\ AP\rightarrow BL}/P_{app\ BL\rightarrow AP}$) (**Table 2**). By comparison of these results with those previousely observed by our group after transepithelial transport by Caco-2 cells of their precursor, hydroxytyrosol (**1**) (*24*), a higher absorption of hydroxytyrosyl alkyl ethers (**2**−**5**) was observed, as indicated by a 1.1−1.7-fold higher P_{app} ratio of these compounds in comparison with their hydrophilic precursor (P_{app} ratio of hydroxytyrosol (**1**) 1.1 ± 0.2) (*24*). Besides, these results are in agreement with the behavior observed for hydroxytyrosyl acetate, which also exhibited a P_{app} ratio 1.5-fold higher than that of its hydrophilic precursor hydroxytyrosol (**1**) (*24*). Previously published data have shown the same correlation between intestinal absorption and lipophilicity (*25*−*28*). Absorption of fumaric acid esters (methyl, ethyl, propyl, and *n*-pentyl) across Caco-2 cell monolayers increased with increasing alkyl ester chain length (*25*). Studying absorption in situ in rat jejunum, ileum, colon, and rectum, Kimura et al. (*26*) observed that the absorption rates of a homologous series of salicylic acid esters increased with increasing acyl chain length (acetyl, propionyl, and butyryl). Houston et al. (*27*) reported the same trend for a homologous series of carbamates in rat tissue using an everted gut technique. An increase in intestinal absorption was observed from methyl- to *n*-butyl esters. However, when the chain length was further increased, absorption rates were reduced. More recently, Tammela et al. (*28*) demonstrated an influence of alkyl chain length on the uptake and transport of synthetic alkyl gallates, with the absorption of medium chain length gallates (*n*-propyl) occurring more rapidly than that of shorter derivatives (*n*-methyl) in Caco-2 cells. However, for the longest chain length assessed (*n*-octyl gallate) no apical to basolateral transport was detected.

Data presented here also show that a portion of the hydroxytyrosyl alkyl ethers is metabolized by phase 2 enzymes during absorption. Monoglucuronides, methylated derivatives, and, for hydroxytyrosyl propyl ether (**4**), methylglucuronides, were identified after incubation with Caco-2/TC7 cells. We provide evidence that methylation was greatest for the least lipophilic compounds (hydroxytyrosyl methyl (**2**) and ethyl (**3**) ethers) and that glucuronidation was greatest for the most lipophilic compounds (hydroxytyrosyl propyl (**4**) and butyl (**5**) ethers), although the preferential metabolic pathways followed by these synthetic polyphenols could be dependent on the concentration reaching the intestine. This behavior is in keeping with the fact that UDP-glucuronosyltransferases (UGTs) are a family of membrane-bound proteins in the endoplasmic reticulum that catalyze glucuronic acid transfer from UDP-glucuronic acid (UDP-GA) to acceptor compounds that are lipophilic in nature and are thus rendered more water-soluble and suitable for excretion (biliary, urinary) from the body (*29*). The observation that the most lipophilic compounds were preferentially glucuronidated may be due to their exhibiting increased accessibility to, or enhanced affinity for, this membrane-bound enzyme. In contrast, catechol-*O*-methyltransferase (COMT) is typically a cytosolic enzyme (*30*), and the enhanced methylation of the most

hydrophilic compounds likely reflects their increased access to and affinity for this enzyme. Comparison of these results with the behavior observed for hydroxytyrosol (**1**) shows that the methylated form of hydroxytyrosol (homovanillyl alcohol) was the only metabolite detected after its incubation with Caco-2 cells, without observation of hydroxytyrosol glucuronide. Thus, the described exclusive methylation of hydroxytyrosol (**1**) by Caco-2 cells was consistent with data reported in the present study, in which methylation was predominant in the less lipophilic compounds assayed.

No sulfated conjugates were identified after incubation of any of the hydroxytyrosyl ethers (**2**−**5**) with Caco-2/TC7 cells. This is notable because it is known that sulfotransferase enzymes (SULT1 and SULT2) are expressed by these cells (*31*, *32*). Furthermore, there are many studies indicating that a variety of phenolic and polyphenolic compounds are efficiently sulfated when exposed to Caco-2 cells (*33*−*35*), although evidence of limited sulfation of hydroxytyrosol (**1**) has also been reported (*36*). It is possible that a low level of sulfation of the hydroxytyrosyl alkyl ethers did occur, but we were not able to detect sulfated metabolites in these experiments. In agreement with these results, no sulfation of hydroxytyrosol (**1**) was detected after its metabolism by enterocyte-like Caco-2 cells (*24*).

The data presented here show that the hydroxytyrosyl alkyl ethers (**2**−**5**) are prone to metabolic reactions such as glucuronidation and methylation during transport across an enterocyte monolayer, but a significant portion of the transported material is not metabolized and would be expected to reach the portal blood unmodified. Thus, the proportions of unconjugated compounds reaching the basolateral compartment after 2 h of incubation were 84, 65, 40, and 37% for hydroxytyrosyl methyl (**2**), ethyl (**3**), propyl (**4**), and butyl ethers (**5**), respectively. With regard to their precursor hydroxytyrosol (**1**), 80% of the material reaching the basolateral compartment was unmetabolized (*24*). These data indicate that the hydroxytyrosyl alkyl ethers (**2**−**5**) as well as hydroxytyrosol (**1**) are taken up by the enterocytes, presumably via passive diffusion, which renders them accessible to intracellular conjugating enzymes with a direct relationship between the lipophilic nature of the tested compound and its metabolization yield. Also, these results suggest a potential for the liver to play an important role in the phase 2 metabolism of these compounds. It is possible that a significant proportion of the initial compounds may completely escape first-pass metabolism and appear in peripheral blood in nonconjugated forms. However, we have observed that these hydroxytyrosyl alkyl ethers are efficiently conjugated by liver cells (*37*), which suggests that the predominant form in human peripheral blood would be conjugates. This may have important consequences because the initial compounds are significantly more lipohilic than the glucuronidated metabolites, or even their precursor hydroxytyrosol (**1**), and are much more likely to accumulate in lipophilic tissues. Nevertheless, the total potential biological impact of the compounds will be due to the sum of the effects of the nonconjugated plus the conjugated forms, and it is important that future research to evaluate the biological activities of these compounds in vitro considers both the unconjugated and the conjugated forms (*38*).

Once the glucuronide and methylated conjugates are formed within the enterocytes, they may diffuse passively or be actively transported out of the cells. The original compounds are sufficiently hydrophobic to facilitate passive diffusion across biological membranes. However, this is not true for glucuronide conjugates, which are rather hydrophilic. We present data indicating that the ratios of apical to basolateral efflux for both the glucuronidated and the methylated metabolites are not close to 1.0 (**Table 3**). Furthermore, the fact that the ratios are substantially lower than 1.0 indicates that basolateral transport is dominant over apical transport. This is true for both the monoglucuronide and methylated conjugates. The actual efflux ratios (ER) observed for the glucuronides and the methylated derivatives (0.02 and 0.08, respectively) indicate that 98% of glucuronides and 92% of methylated derivatives are transported to the basolateral side, with only a tiny fraction of either of them transported to the apical side. These results are in line with the preferential efflux across the basolateral membrane observed for hydroxytyrosol (**1**) and its methyl conjugate (*24*).

Finally, some of the most relevant in vivo activities of natural phenols are related to inhibition of oxygenases, such as COX and LOX. This type of activity is certainly facilitated by their amphiphilic nature, allowing interactions with enzymatic proteins. In this sense, recently Procopio et al. (*39*) observed that homologous derivatives from oleuropein and hydroxytyrosol have significant inhibitory activity on COX-1 and COX-2, highlighting the greater inhibitory activity of paracetylated lipophilic derivatives versus paracetylated hydroxytyrosol. With these considerations taken into account, it is predictable that this new batch of lipophilic hydroxytyrosol derivatives presents higher activity related to inhibition of oxygenases, among others.

In summary, the data presented here showed that synthetic hydroxytyrosyl ethers (**2**−**5**) derived from hydroxytyrosol (**1**) are efficiently absorbed across and partially metabolized by intestinal epithelial cell monolayers, in keeping with their lipophilic nature. Glucuronides and methylated derivatives, but not sulfates, were detected. In addition, between 40 and 85% of the apically applied compound escaped metabolism during transport to the basolateral side, suggesting a remarkable ability of the unmetabolized compunds to reach the bloodstream.

LITERATURE CITED

(1) Rietjens, S. J.; Bast, A.; Haenen, G. R. M. M. New insights into controversies on the antioxidant potential of the olive oil antioxidant hydroxytyrosol. *J. Agric. Food Chem.* **2007**, *55*, 7609−7614.

(2) Carluccio, M. A.; Siculella, L.; Ancora, M. A.; Massaro, M; Scoditti, E.; Storelli, C; Visioli, F.; Distante, A.; De Caterina, R. Olive oil and red wine antioxidant polyphenols inhibit endothelial activation: antiatherogenic properties of Mediterranean diet phytochemicals. *Arterioscler. Thromb. Vasc. Biol.* **2003**, *23*, 622−629.

(3) Dell'Agli, M.; Maschi, O.; Galli, G. V.; Fagnani, R.; Dal Cero, E.; Caruso, D.; Bosisio, E. Inhibition of platelet aggregation by olive oil phenols via cAMP-phosphodiesterase. *Br. J. Nutr.* **2008**, *99*, 945−951.

(4) Bitler, C. M.; Viale, T. M.; Damaj, B.; Crea, R. Hydrolyzed olive vegetation water in mice has anti-inflammatory activity. *J. Nutr.* **2005**, *135*, 1475−1479.

(5) Fabiani, R.; Fuccelli, R.; Pieravanti, F.; De Bartolomeo, A.; Morozzi, G. Production of hydrogen peroxide is responsible for the induction of apoptosis by hydroxytyrosol on HL60 cells. *Mol. Nutr. Food Res.* **2009**, *53*, 887−896.

(6) Guichard, C.; Pedruzzi, E.; Fay, M.; Marie, J. C.; Braut-Boucher, F.; Daniel, F.; Grodet, A.; Gougerot-Pocidalo, M. A.; Chastre, E.; Kotelevets, L.; Lizard, G.; Vandewalle, A.; Driss, F.; Ogier-Denis, E. Dihydroxyphenylethanol induces apoptosis by activating serine/threonine protein phosphatise PP2A and promotes the endoplasmic reticulum stress response in human colon carcinoma cells. *Carcinogenesis* **2006**, *27*, 1812−1827.

(7) Goya, L.; Mateos, R.; Bravo, L. Effect of the olive oil phenol hydroxytyrosol on human hepatoma HepG2 cells. Protection against oxidative stress induced by tert-butylhydroperoxide. *Eur. J. Nutr.* **2007**, *46*, 70−78.

(8) Rietjens, S. J.; Bast, A.; Vente, J.; Haenen, G. R. M. M. The olive oil antioxidant hydroxytyrosol efficiently protects against the oxidative stress-induced impairment of the NO response of isolated rat aorta. *Am. J. Physiol. Heart Circ. Physiol.* **2007**, *292*, 1931−1936.

(9) Martín, M. A.; Ramos, S.; Granado-Serrano, A. B.; Rodríguez-Ramiro, I.; Trujillo, M.; Bravo, L.; Goya, L. The olive oil phenol hydroxytyrosol induces antioxidant/detoxificant enzymes activity and Nrf2 translocation via ERKs and PI3K/AKT pathways in HepG2 cells. *Mol. Nutr. Food Res.* **2010**, *54*, 956−966.
(10) Caruso, D.; Visioli, F.; Patelli, R.; Galli, C.; Galli, G. Urinary excretion of olive oil phenols and their metabolites in humans. *Metab., Clin. Exp.* **2001**, *50*, 1426−1428.
(11) Tuck, K. L.; Hayball, P. J.; Stupans, I. Structural characterization of the metabolites of hydroxytyrosol, the principal phenolic component in olive oil, in rats. *J. Agric. Food Chem.* **2002**, *50*, 2404−2409.
(12) Miró-Casas, E.; Covas, M.-I.; Farré, M.; Fito, M.; Ortuño, J.; Weinbrenner, T.; Roset, P.; de la Torre, R. Hydroxytyrosol disposition in humans. *Clin. Chem.* **2003**, *49*, 945−952.
(13) Visioli, F.; Galli, C.; Bornet, F.; Mattei, A.; Patelli, R.; Galli, G.; Caruso, D. Olive oil phenolics are dose-dependently absorbed in humans. *FEBS Lett.* **2000**, *468*, 159−160.
(14) De la Torre, R. Bioavailability of olive oil phenolic compounds in humans. *Inflammopharmacology* **2008**, *16*, 245−247.
(15) Madrona, A.; Pereira-Caro, G.; Mateos, R.; Rodriguez, G.; Trujillo, M.; Fernandez-Bolanos, J.; Espartero, J. L. Synthesis of hydroxytyrosyl allkyl ethers from olive oil waste waters. *Molecules* **2009**, *14*, 1762−1772.
(16) Pereira-Caro, G.; Madrona, A.; Bravo, L.; Espartero, J. L.; Alcudia, F.; Cert, A.; Mateos, R. Antioxidant activity evaluation of alkyl hydroxytyrosyl ethers, a new class of hydroxytyrosyl derivatives. *Food Chem.* **2009**, *115*, 86−91.
(17) Espartero, J. L.; Pereira-Caro, G.; Madrona, A.; Bravo, L.; Trujillo, M.; Alcudia, F.; Cert, A.; Mateos, R. Preparation and antioxidant activity of tyrosyl and homovanillyl ethers. *Book II of Proceedings of Euro Food Chem XV*; Sorensen, H., Sorensen, S., Sorensen, A. D., Sorensen, J. C., Andersen, K. E., Bjergegaard, C., Moller, P., Eds.; University of Copenhagen: Copenhagen, Denmark, 2009; pp 193−196, ISBN 978-87-993033-5-9.
(18) Mateos, R.; Goya, L.; Bravo, L. Uptake and metabolism of hydroxycinnamic acids (chlorogenic, caffeic, and ferulic acids) by HepG2 cells as a model of the human liver. *J. Agric. Food Chem.* **2006**, *54*, 8724−8732.
(19) Graham, J. M., Rickwood, D., Eds. *Subcellular Fractionation − A Practical Approach*; Oxford University Press: Oxford, U.K., 1997; pp 205−242.
(20) Mateos, R.; Goya, L.; Bravo, L. Metabolism of the olive oil phenols hydroxytyrosol, tyrosol, and hydroxytyrosyl acetate by human hepatoma HepG2 cells. *J. Agric. Food Chem.* **2005**, *53*, 9897−9905.
(21) Artursson, P.; Karlsson, J. Correlation between oral drug absorption in humans and apparent drug permeability coefficients in human intestinal epithelial (Caco-2) cells. *Biochem. Biophys. Res. Commun.* **1991**, *175*, 880−885.
(22) Covas, M. I.; de la Torre, K.; Farré-Albaladejo, M.; Kaikkonen, J.; Fitó, M.; López-Sabater, C.; Pujadas-Bastardes, M. A.; Joglar, J.; Weinbrenner, T.; Lamuela-Raventós, R. M.; de la Torre, R. Postprandrial LDL phenolic content and LDL oxidation are modulated by olive oil phenolic compounds in humans. *Free Radical Biol. Med.* **2006**, *40*, 608−616.
(23) Vissers, M. N.; Zock, P. L.; Roodenburg, A. J.C.; Leenen, R.; Katan, M. B. Olive oil phenols are absorbed in humans. *J. Nutr.* **2002**, 409−417.
(24) Mateos, R.; Pereira-Caro, G.; Saha, S.; Cert, R.; Redondo-Horcajo, M.; Bravo, L.; Kroon, P. A. Acetylation of hydroxytyrosol enhances its transport across differentiated CaCo-2 cell monolayers. *Food Chem.* In press. DOI information: 10.1016/j.foodchem.2010.09.054.
(25) Werdenberg, D.; Joshi, R.; Wolffram, S.; Merkle, H. P.; Langguth, P. Presystemic metabolism and intestinal absorption of antipsoriatic fumaric acid esters. *Biopharm. Drug Dispos.* **2003**, *24*, 259−273.
(26) Kimura, T.; Sudo, K.; Kanzaki, Y. Durg absorption from large intestine: physicochemical factors governing drug absorption. *Biol. Pharm. Bull.* **1994**, *17*, 327−333.
(27) Houston, J. B.; Upshall, D. G.; Birdges, J. W. A re-evaluation of the importance of partition coefficients in the gastrointestinal absorption of a nutrient. *J. Pharmacol. Exp. Ther.* **1974**, *189*, 244−254.
(28) Tammela, P.; Laitinen, L.; Galkin, A.; Wennbert, T.; Heczko, R.; Vuorela, H.; Slotte, J. P.; Vuorela, P. Permeability characteristics and membrane affinity of flavonoids and alkyl gallates in Caco-2 cells and in phospholipid vesicles. *Arch. Biochem. Biophys.* **2004**, *425*, 193−199.
(29) Tukey, R. H.; Strassburg, C. P. Human UDP-glucuronosyltransferases: metabolism, expression and disease. *Annu. Rev. Pharmacol. Toxicol.* **2000**, *40*, 581−616.
(30) Tenhunen, J.; Salminen, M.; Lundstrom, K.; Kiviluoto, T.; Savolainen, R.; Ulmanen, I. Genomic ortanization of the human catechol *O*-methyltransferase gene and its expression from two distinct promoters. *Eur. J. Biochem.* **1994**, *223*, 1049−1059.
(31) Chen, Y.; Huang, C.; Zhou, T.; Chen, G. Genistein induction of human sulfotransferases in HepG2 and Caco-2 cells. *Basic Clin. Pharmacol. Toxicol.* **2008**, *103*, 553−559.
(32) Meinl, W.; Ebert, B.; Glatt, H.; Lampen, A. Sulfotransferase forms expressed in human intestinal Caco-2 and TC7 cells at varying stages of differentiation and role in benzo[a]pyrene metabolism. *Drug Metab. Dispos.* **2008**, *36*, 276−283.
(33) Barrington, R.; Wiliamson, G.; Bennett, R. N.; Davis, B. D.; Brodbelt, J. S.; Kroon, P. A. Absorption, conjugation and efflux of the flavonoides, kaempferol and galangin, using the intestinal Caco-2/TC7 cell model. *J. Funct. Foods* **2009**, *1*, 74−87.
(34) Kern, S. M.; Bennett, R. N.; Needs, P. W.; Mellon, F. A.; Kroon, P. A.; Garcia-Conesa, M. T. Characterization of metabolites of hydroxycinnamates in the in vitro model of human small intestinal epithelium Caco 2 cells. *J. Agric. Food Chem.* **2003**, *51*, 7884−7891.
(35) Kaldas, M. I.; Walle, K.; Walle, T. Resveratrol transport and metabolism by human intestinal Caco-2 cells. *J. Pharm. Pharmacol.* **2003**, *55*, 307−312.
(36) Soler, A.; Romero, M. P.; Macia, A.; Saha, S.; Furniss, C. S. M.; Kroon, P. A.; Motilva, M. J. Digestion stability and evaluation of the metabolism and transport of olive oil phenols in the human small-intestinal epityhelial Caco-2/TC7 cell line. *Food Chem.* **2010**, *119*, 703−714.
(37) Pereira-Caro, G.; Bravo, L.; Madrona, A.; Espartero, J. L.; Mateos, R. Uptake and metabolism of new synthetic lipophilic derivatives, hydroxytyrosyl ethers, by human hepatoma HepG2 cells. *J. Agric. Food Chem.* **2010**, *58*, 798−806.
(38) Kroon, P. A.; Clifford, M. N.; Crozier, A.; Day, A. J.; Donovan, J. L.; Manach, C.; Williamson, G. How should we assess the effects of exposure to dietary polyphenols in vitro? *Am. J. Clin. Nutr.* **2004**, *80*, 15−21.
(39) Procopio, A.; Alcaro, S.; Nardi, M.; Oliverio, M.; Ortuso, F.; Sacchetta, P.; Pieragostino, D.; Sindona, G. Synthesis, biological evaluation and molecular modelling of oleuropein and its semisynthetic derivatives as cyclooxygenase inhibitors. *J. Agric. Food Chem.* **2009**, *57*, 11161−11167.

Received for review May 22, 2010. Revised manuscript received August 25, 2010. Accepted September 13, 2010. This work was supported by Projects AGL2007-64042, AGL2007-66373-C04/ALI, and CSD2007-00063 from the Consolider-Ingenio Program of the Spanish Ministry of Science and Innovation (CICYT), Grant RTA2007-000036-00-00 from the National Research Institute of Food, Agriculture and Technology (INIA), Contract 110105090014 with CSIC-IFAPA, and by the Biotechnology & Biological Sciences Research Council, U.K. (P.A.K., S.S.). G.P.-C. is a predoctoral fellow of the National Research Institute of Food, Agriculture and Technology (INIA). R.M. thanks the Spanish Ministry of Education for a José Castillejo mobility grant.